

Short communication

Differences in physical phenomena governing laser machining of structural ceramics

Anoop N. Samant, Narendra B. Dahotre*

Department of Materials Science and Engineering, The University of Tennessee, Knoxville, TN 37996, United States

Received 18 August 2008; received in revised form 23 September 2008; accepted 9 November 2008

Available online 3 December 2008

Abstract

Several structural ceramics such as alumina, silicon nitride, silicon carbide and magnesia were machined using a pulsed Nd:YAG laser. Laser processing conditions and temperature dependent thermo-physical properties govern the physical phenomena that machine these ceramics. Melting, dissociation and evaporation are some of the vital mechanisms associated with material removal. Discrimination and incorporation of these physical processes into a hydrodynamic machining model to predict different machining parameters was conducted. The model provides an outstanding tool for advance prediction of thermal energy and time required for machining desired depth of material.

© 2008 Elsevier Ltd and Techna Group S.r.l. All rights reserved.

Keywords: D. Al_2O_3 ; D. Si_3N_4 ; D. SiC; D. MgO

1. Introduction

Exceptional properties like high hardness, high thermal resistance and chemical stability have increased the use of structural ceramics such as alumina (Al_2O_3), silicon carbide (SiC), silicon nitride (Si_3N_4) and magnesia (MgO) for several electronic, automotive and medical applications [1]. Al_2O_3 is used in making seals, valves, medical implants, and as a substrate in hybrid circuits. Piston rings, bearings, cams are made by machining Si_3N_4 while MgO is used in brake linings, thermocouple housings and in thin film semi-conductors. SiC is also gaining popularity for high temperature, high frequency and high power applications. Hard and brittle nature of these ceramics pose a hindrance in the use of traditional methods based on mechanical grinding and fracturing for machining them. Recently, Laser Machining (LM) has transpired to be one of the widely desired machining techniques on account of its contact less processing, low production costs, efficient material utilization and automation [2–5]. This study aims at understanding the physical phenomena behind the material removal process during machining the above mentioned structural ceramics by a JK 701 pulsed Nd:YAG laser (1064 nm

wavelength). The intention of this paper is just to discriminate various mechanisms such as melting, dissociation and evaporation which could be responsible for machining of the different structural ceramics. However, the details of the physical processes and computational results associated with machining of each individual ceramic are separately described elsewhere [6–9].

2. Laser–ceramic interaction

Once the laser beam is incident on the ceramic surface, absorption, reflection, refraction, transmission, and scattering are the different physical phenomena that take place. The majority of the energy is absorbed and this absorption depends on the wavelength and spectral absorptivity characteristics of the material being machined [10]. For machined cavities with high aspect ratios as considered in this study, the multiple beam reflections along the wall of the cavity also influence the energy absorption and 100% of the energy is immediately absorbed [11].

2.1. Temporal evolution

The laser energy converted into heat conducts into the material according to Fourier's second law of heat transfer (Eq. (1)), and simultaneously radiates (Eq. (2)) and convects

* Corresponding author. Tel.: +1 865 974 3609; fax: +1 865 974 4115.

E-mail address: ndahotre@utk.edu (N.B. Dahotre).

(Eq. (3)) from the surface [12].

$$\frac{\partial T(x, y, z, t)}{\partial t} = \alpha(T) \left[\frac{\partial^2 T(x, y, z, t)}{\partial x^2} + \frac{\partial^2 T(x, y, z, t)}{\partial y^2} + \frac{\partial^2 T(x, y, z, t)}{\partial z^2} \right] \quad (1)$$

where $k(T)$ and $C_p(T)$ are variations in thermal conductivity and specific heat as a function of temperature, ρ is density of ceramic, T is temperature field, t is time and x , y and z are spatial directions.

$$\begin{aligned} -k(T) \left(\frac{\partial T(x, y, 0, t)}{\partial x} + \frac{\partial T(x, y, 0, t)}{\partial y} + \frac{\partial T(x, y, 0, t)}{\partial z} \right) \\ = \frac{4\delta a Q}{\pi d^2} - \varepsilon \sigma (T(x, y, 0, t)^4 - T_0^4) \end{aligned} \quad (2)$$

$\delta = 1$ if $0 \leq t \leq t_{on}$; $\delta = 0$ if $t > t_{on}$

where ε is emissivity for thermal radiation, Q is incident beam power, d is beam diameter, T_0 is ambient temperature, t_{on} is the pulse ON time, σ is Stefan-Boltzman constant ($5.67 \times 10^{-8} \text{ W/m}^2 \text{ K}^4$) and a is absorptivity of the material. In the present case, the values of absorptivity were obtained from previously published references in the open literature. Although it is very difficult in an extremely short duration high energy density dynamic process like laser-material interaction to accurately conduct in situ absorptivity measurements, efforts are going on in parallel for in situ measurement of actual absorptivity values under laser processing conditions similar to the ones employed in the present work. The term δ takes a value of 1 when the time, t is less than t_{on} and it is 0 when the time, t exceeds t_{on} . Thus the value of δ depends on the time, t and ensures that the energy is input to the system only during the pulse on-time and cuts off the energy supply during the following pulse off-time.

$$\begin{aligned} -k(T) \left(\frac{\partial T(x, y, D, t)}{\partial x} + \frac{\partial T(x, y, D, t)}{\partial y} + \frac{\partial T(x, y, D, t)}{\partial z} \right) \\ = h(T(x, y, D, t) - T_0) \end{aligned} \quad (3)$$

where D is the thickness of the ceramic being machined and $h(T)$ is the heat transfer coefficient as a function of temperature. The temperature rise and fall during the ON and OFF time, respectively, also affect the temporal and spatial evolution of temperature within the ceramic body which in turn influences the material removal mechanism [13] (Eq. (4 and 5)).

$$\begin{aligned} T'_i = T_i + (T_0 - T_i) \\ \times \left[1 - \left[\exp \frac{h(T)^2 \alpha(T) t_{off}}{k(T)^2} \right] \left[1 - \operatorname{erf} \left(\frac{h(T) \sqrt{\alpha(T) t_{off}}}{k(T)} \right) \right] \right] \end{aligned} \quad (4)$$

where T_i is the temperature during heating of pulse i , t_{off} is the OFF time between successive pulses and $\operatorname{erf}()$ is the error function. The term $\alpha(T)$ is the temperature dependent thermal diffusivity of the material given by $k(T)/\rho C_p(T)$.

$$T_i = T'_{i-1} + \frac{8aQ}{\pi d^2} \frac{\sqrt{\alpha(T) t_{on}/\pi}}{k(T)} \quad (5)$$

where T'_{i-1} is the temperature during cooling of the earlier pulse predicted from Eq. (4) above.

2.2. Governing physical mechanisms

When the surface temperature reaches the melting point of the ceramic, material removal occurs by melting and the solid-liquid interface can be interpreted by tracing the melting point in the temperature versus depth plots. As the surface temperature further increases with pulse time or laser intensity and reaches the vaporization point of the material, material removal takes place by evaporation instead of melting. The rate of material loss at the surface ($\text{kg/m}^2 \text{ s}$) due to evaporation is given by [14]:

$$\dot{m}_{\text{evaporated}} = p(T_s) \left[\frac{m_v}{2\pi k T_s} \right]^{1/2} \quad (6)$$

where T_s is the surface temperature, k is the Boltzmann constant ($1.38065 \times 10^{-23} \text{ J/K}$), m_v is mass of the vapor molecule, and $p(T_s)$ is the saturation pressure given by the Clausius-Clapeyron equation. The evolving vapor from the surface applies recoil pressure on the surface (Eq. (7)) which plays an important role in material removal in molten state during machining of certain ceramics as seen later [15].

$$\frac{\pi d^2 p_{\text{recoil}}}{4aQ} = \frac{1.69}{\sqrt{L_v}} \left(\frac{b}{1 + 2.2b^2} \right) \quad (7)$$

where $b^2 = kT_s/m_v L_v$, and L_v is the latent heat of vaporization. Even though thermo-physical properties mentioned above such as thermal conductivity, specific heat, heat transfer coefficient and thermal diffusivity vary with temperature, the latent heat of vaporization is a constant value independent of temperature.

Based on the thermodynamic conditions prevalent during laser machining, certain ceramics dissociate/decompose into various stoichiometric/non-stoichiometric species that are expelled/removed during the machining process. Assuming the machined cavities with minimum taper to have a cylindrical cross-section of volume $V = \pi d^2 z/4$ (equivalent to $N = V/22.4 \times 10^{-3} \text{ mol}$), the loss of energy corresponding to dissociation of this volume of machined cavity is estimated by $E_{\text{dissociation}} = \Delta G \times N$, where ΔG is Gibbs free energy and z is depth of machined cavity. This dissociation energy loss reduces the effective laser energy available in subsequent pulses and thus the corresponding temperature. As described below, a combination of the different physical processes mentioned above affect the machining of a certain ceramic rather a single predominant process (Table 1).

3. Machining of structural ceramics

Structural ceramics such as alumina (Al_2O_3), silicon nitride (Si_3N_4), silicon carbide (SiC) and magnesia (MgO) were machined using a JK 701 pulsed Nd:YAG laser. Processing conditions and governing physical phenomena for machining of these ceramics are only briefly discussed here for the sole purpose of comparison in this section. As mentioned before,

Table 1

Governing mechanisms in some structural ceramics (✓—phenomena present; ✗—phenomena not present).

| Physical Process ↓ | Material → | O ₃ | Si ₃ N ₄ | SiC | MgO |
|--------------------|------------|----------------|--------------------------------|-----|-----|
| Melting | | ✓ | ✓ | ✓ | ✗ |
| Dissociation | | ✓ | ✓ | ✓ | ✓ |
| Evaporation | | ✓ | ✓ | ✓ | ✓ |

however, detailed analysis of the machining mechanisms in these ceramics has already been conducted by Samant and Dahotre and separately presented elsewhere [6–9].

3.1. Alumina

At a pulse energy of 4 J, repetition rate of 20 Hz and pulse width of 0.5 ms, 5, 10, 20 and 30 pulses were required for machining depths of 0.26, 0.56, 3.23, and 4.0 mm in Al₂O₃ (Fig. 1a) [6]. AlO_(g), Al_(l), Al_(g), Al₂O_(g) and AlO_{2(g)} are some of the species formed due to the dissociation of Al₂O₃ [16]. Recoil pressure provoked expulsion of the liquid phase formed during the dissociation process (most likely by reaction in Eq. (8)) is responsible for laser machining in alumina.



Moreover, there is some loss of material due to evaporation (Eq. (6)) and the machining in alumina is a combined effect of melt expulsion, dissociation and evaporation.

3.2. Silicon nitride

For the same set of laser processing parameters as used for machining alumina, 3, 6, 10 and 20 pulses were able to machine depths of 0.92, 1.13, 1.69 and 3.5 mm, respectively, in Si₃N₄ (Fig. 1b) [7]. The dissociation/sublimation of Si₃N₄ into Si liquid and N₂ gas (Eq. (9) [17]) at the sublimation temperature of Si₃N₄ followed by the expulsion of liquid silicon by evaporation induced recoil pressure (Eq. (7)) was proposed as the material removal mechanism.



Evaporation also assists in material removal and melting, dissociation and evaporation together lead to machining in Si₃N₄ [7].

3.3. Silicon carbide

Using a pulse energy of 6 J, pulse duration of 0.5 ms, and repetition rate of 50 Hz, a through cavity was machined in a 2 mm thick SiC plate in approximately 25 pulses while it took about 125 pulses to machine through the entire thickness of a 3 mm thick plate (Fig. 1c) [8]. Decomposition of SiC may produce several species such as Si_(g), Si_{2(g)}, SiC_{2(g)}, Si_(l), C_(s), Si_(s), Si₂C_(g), C_(g), and Si_{3(g)}. The most likely reaction to produce liquid species available for expulsion is:

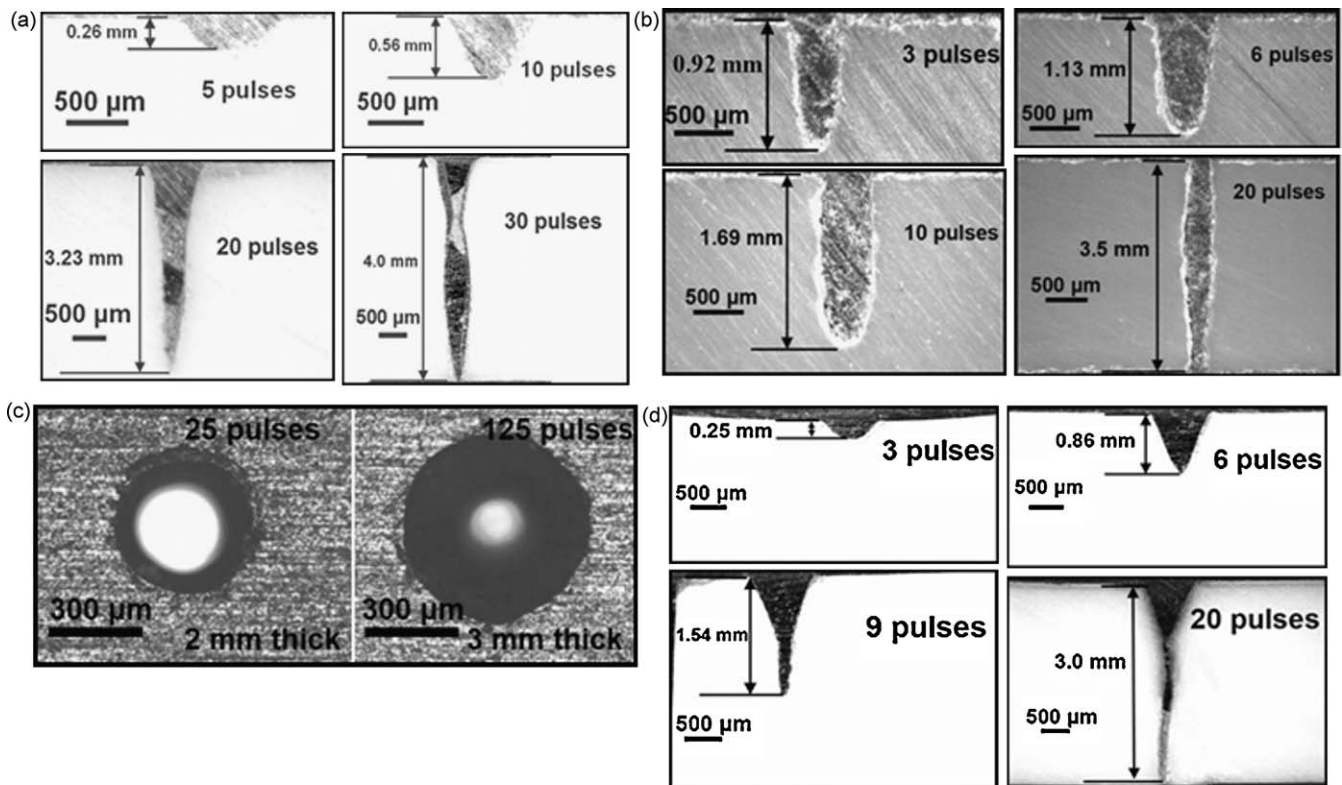


Fig. 1. Laser machining of (a) Al₂O₃, (b) Si₃N₄, (c) SiC and (d) MgO.

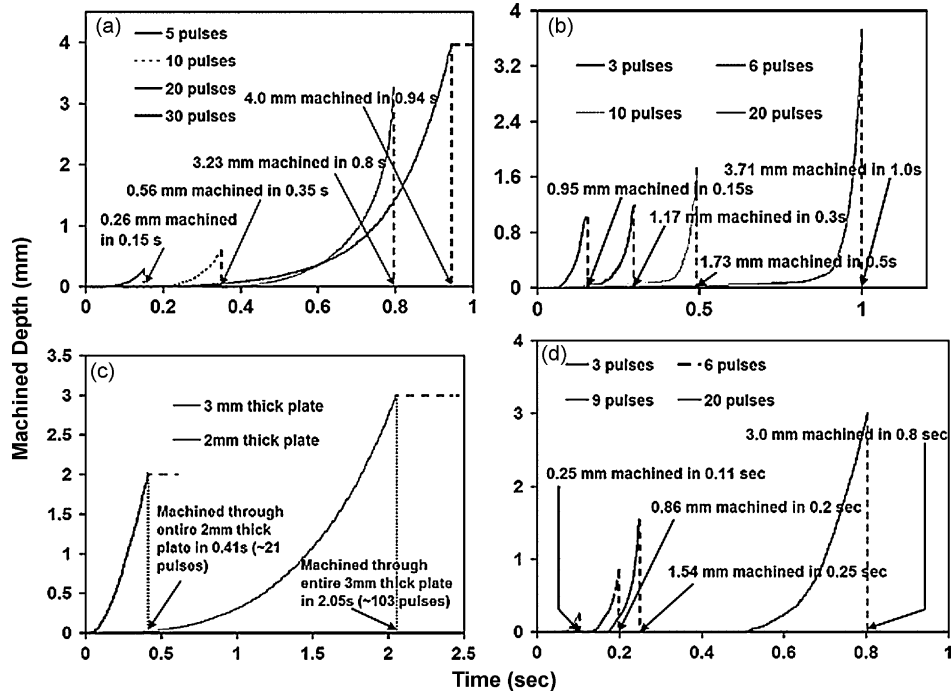


Fig. 2. Machined depth evolution for (a) Al_2O_3 , (b) Si_3N_4 , (c) SiC and (d) MgO .

Similar to alumina and silicon nitride, some loss of material also occurs due to evaporation and a combination of melting, dissociation and evaporation contributes to machining in silicon carbide.

3.4. Magnesia

Finally, under the combination of a pulse energy of 4 J, pulse width of 0.5 ms and a repetition rate of 20 Hz, several pulses (3, 6, 9 and 20) were applied to the MgO surface and depths of 0.25, 0.86, 1.54 and 3.0 mm were machined (Fig. 1d) [9]. MgO dissociates as per the following reaction [18]:



The melting and vaporization temperatures of magnesium (922 K and 1363 K, respectively) being less than the dissociation temperature of MgO (3123 K), the solid magnesium formed due to the dissociation reaction (Eq. (11)) immediately evaporates and material losses in MgO take place solely by evaporation. Dissociation along with evaporation of the ceramic exposed to laser fluence causes material removal in MgO . This mechanism is in contrast to the machining of Al_2O_3 , Si_3N_4 and SiC using the same laser based technique. As the material evaporates, the removed material (vapor) exerts a force over the machined area and drives out the material. This force acting upwards is proportional to the laser fluence (energy per unit area) essential for machining a certain depth, z and is given by:

$$\text{Vapor pressure} = \frac{\text{Laser fluence}}{\text{Machined depth}} \quad (12)$$

This vapour pressure (Eq. (12)) is different from the recoil pressure mentioned above (Eq. (7)) and is exerted only during the machining of ceramics such as MgO where the entire material goes directly into vaporization without any melting involved. On the other hand, recoil pressure (Eq. (7)) is experienced in those ceramics in which machining takes place by a combination of melting and evaporation. Simultaneously,

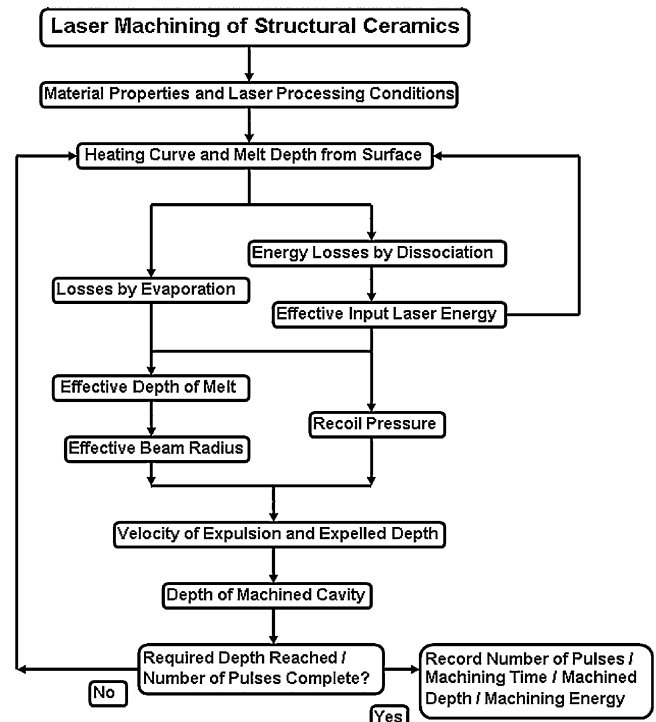


Fig. 3. Stepwise procedure for prediction of machining parameters.

the gravitational pull (ρgz , where g is acceleration due to gravity) acts downwards and the extent of cavity formation is governed by these counterbalancing pressures. A clean cavity is formed when the vapour pressure exceeds the gravitational pull.

4. Computational model

The above described physical processes along with the material properties and laser processing conditions can be incorporated into a computational model for prediction of several machining parameters such as machining time, number of pulses, dimensions of machined cavity and machining energy. In light of this, an ab initio physical model was developed by Samant and Dahotre and used for predicting the number of pulses and corresponding time required for machining a certain depth in Al_2O_3 (Fig. 2a) [6] and for estimating depth of machined cavity when a certain number of pulses were applied to Si_3N_4 (Fig. 2b) [7]. The model was also applied for advance prediction of number of pulses and corresponding energy necessary for machining SiC ceramic (Fig. 2c) [8] and to determine the number of pulses and corresponding time required for machining a certain depth in MgO (Fig. 2d) [9].

As the details of modeling have been elaborately explained by Samant and Dahotre in references [6] to [9], only a general flow chart for predicting the desired machining parameters is represented in Fig. 3. The nature of the structural ceramic governs the physical phenomena that can be incorporated into the mathematical model and it was found that the predictions were within acceptable range of the actual observations.

5. Conclusion

This study demonstrates the feasibility of lasers in machining some of the commonly used structural ceramics and establishes the fact that the material removal mechanism depends on the type of ceramic. Based on this concept, a computational tool was developed that was capable of advance predictions of the machining parameters. It was observed that even though the laser processing conditions were identical for most of the ceramics, the depth of the machined cavity was different for all of them because the machining process was a function of the thermo-physical properties of the ceramic such as thermal conductivity, specific heat, latent heat and density. Furthermore, this study is different from earlier work such as that of Salonitis et al. [13] who considered the machining mechanism as comprised of only melting and subsequent material removal by melt expulsion and Atanasov et al. [19] who thought of machining as a single step material evaporation without any melting.

References

- [1] I.P. Tuerstley, A. Jawaid, I.R. Pashby, Review: various methods of machining advanced ceramic materials, *J. Mater. Process. Technol.* 42 (4) (1994) 377–390.
- [2] G. Chryssolouris, *Laser Machining: Theory and Practice*, Springer-Verlag, New York, 1991.
- [3] K. Salonitis, P. Stavropoulos, A. Stournaras, G. Chryssolouris, CO_2 Laser cutting of aluminium, in: *Proceedings of the 5th Laser Assisted Net Shape Engineering*, Erlangen, Germany, 2007, pp. 825–835.
- [4] P. Stavropoulos, K. Salonitis, A. Stournaras, K. Euthimiou, G. Chryssolouris, Molecular dynamics simulation of laser ablation of iron, in: *Proceedings of the 10th CIRP International Workshop on Modeling of Machining Operations*, Calabria, Italy, 2007, pp. 549–553.
- [5] A. Stournaras, K. Salonitis, P. Stavropoulos, G. Chryssolouris, Finite element thermal analysis of pulsed laser drilling process, in: *Proceedings of the 10th CIRP International Workshop on Modeling of Machining Operations*, Calabria, Italy, 2007, pp. 563–570.
- [6] A.N. Samant, N.B. Dahotre, Computational predictions in single dimensional laser machining of alumina, *Int. J. Mach. Tools Manuf.* 48 (2008) 1345–1353.
- [7] A.N. Samant, N.B. Dahotre, Ab initio physical analysis of single dimensional laser machining of silicon nitride, *Adv. Eng. Mater.* 10 (2008) 978–981.
- [8] A.N. Samant, C. Daniel, R.H. Chand, C.A. Blue, N.B. Dahotre, Computational approach to photonic drilling of silicon carbide, *Int. J. Adv. Manuf. Technol.*, under review.
- [9] A.N. Samant, N.B. Dahotre, An integrated computational approach to single dimensional laser machining of magnesia, *Opt. Lasers Eng.*, in press, doi:10.1016/j.optlaseng.2008.10.001.
- [10] M.U. Islam, G. Campbell, Laser machining of ceramics: a review, *Mater. Manuf. Processes*. 8 (6) (1993) 611–630.
- [11] H. Ki, P.S. Mohanty, J. Mazumder, Multiple reflection and its influence on keyhole evolution, *J. Laser Appl.* 14 (2002) 39–45.
- [12] S.P. Harimkar, A.N. Samant, N.B. Dahotre, Temporally evolved recoil pressure driven melt infiltration during laser surface modifications of porous alumina ceramic, *J. Appl. Phys.* 101 (2007) DOI: 054911.
- [13] K. Salonitis, A. Stournaras, G. Tsoukantas, P. Stavropoulos, G. Chryssolouris, A theoretical and experimental investigation on limitations of pulsed laser drilling, *J. Mater. Process. Technol.* 183 (1) (2007) 96–103.
- [14] W.W. Duley, *Laser Welding*, Wiley Interscience Publication, New York, NY, 1998.
- [15] V.V. Semak, G.A. Knorovsky, D.O. MacCallum, R.A. Roach, Effect of surface tension on melt pool dynamics during laser pulse interaction, *J. Phys. D: Appl. Phys.* 39 (2006) 590–595.
- [16] P.V. Ananthapadmanabhan, T.K. Thiyagarajan, K.P. Sreekumar, N. Venkatramani, Formation of nano-sized alumina by in-flight oxidation of aluminium powder in a thermal plasma reactor, *Scr. Mater.* 50 (1) (2004) 143–147.
- [17] J.P. Murray, G. Flamant, C.J. Roos, Silicon solar-grade silicon production by solar dissociation of Si_3N_4 , *Sol. Energy* 80 (10) (2006) 1349–1354.
- [18] T. Yabe, M.S. Mohamed, S. Uchida, C. Baasandash, Y. Sato, M. Tsuji, Y. Mori, Noncatalytic dissociation of MgO by laser pulses towards sustainable energy cycle, *J. Appl. Phys.* 101 (2007) DOI: 10.1063/1.2743730.
- [19] P.A. Atanasov, E.D. Eugenieva, N.N. Nedialkov, Laser drilling of silicon nitride and alumina ceramics: a numerical and experimental study, *J. Appl. Phys.* 89 (2001) DOI: 10.1063/1.1334367.